Composites Science and Technology 71 (2011) 315–325

Contents lists available at ScienceDirect

Composites Science and Technology

journal homepage: www.elsevier.com/locate/compscitech

Compressibility of carbon woven fabrics with carbon nanotubes/nanofibres grown on the fibres

Stepan V. Lomov [a,*], Larissa Gorbatikh [a], Željko Kotanjac [b], Vitaly Koissin [c], Matthieu Houlle [d], Olivier Rochez [d], Mehmet Karahan [e], Luca Mezzo [d], Ignaas Verpoest [a]

[a] Department of Metallurgy and Materials Engineering, Katholieke Universiteit Leuven, Kasteelpark Arenberg, 44, B-3001 Leuven, Belgium
[b] Faculty of Science and Technology, University of Twente, P.O. Box 217, 7500 AE Enschede, The Netherlands
[c] Department of Design, Production and Management, University of Twente, P.O. Box 217, 7500 AE Enschede, The Netherlands
[d] Department of Research and Development, Nanocyl S.A., Rue de l' Essor 4, B-5060 Sambreville, Belgium
[e] Uludag University, Vocational School of Technical Sciences, Gorukle, Bursa, Turkey

ARTICLE INFO

Article history:
Received 3 September 2010
Received in revised form 19 November 2010
Accepted 25 November 2010
Available online 30 November 2010

Keywords:
A. Nano composites
A. Fabrics/textiles
B. Mechanical properties
D. Compaction

ABSTRACT

Growth of carbon nanotubes (CNT) or carbon nano-fibres (CNF) on carbon fibrous substrates is a way to increase the fracture toughness of fibre reinforced composites (FRC), with encouraging results reported in the recent years. If these nano-engineered FRC (nFRC) are destined to leave laboratories and enter industrial-scale production, a question of adapting the existing composite manufacturing methods will arise. The paper studies compressibility of woven carbon fibre performs (two types of fabrics) with CNT/CNF grown on the fibres using the CVD method. The results include pressure vs thickness and pressure vs fibre volume fraction diagrams for one and four layers of the fabric. Morphology of the nFRC is studied with SEM. It is shown that the pressure needed to achieve the target fibre volume fraction of the preform increases drastically (for example, from 0.05 MPa to more than 0.5 MPa for a fibre volume fraction of 52%) when CNT/CNF are grown on it. No change in nesting of the fabric plies is noticed. The poor compressibility can lower the achievable fibre volume fraction in composite for economical vacuum assisted light-RTM techniques and increase the pressure requirements in autoclave processing.

1. Introduction

Nano-tailoring of fibre reinforced composites (FRC) was attempted soon after the discovery of carbon nanotubes (CNT). Introducing CNT or carbon nano-fibres (CNF) as an additional hierarchical level of heterogeneity in FRC (nano–micro–meso–macro) is intended to solve the intrinsic controversy of FRC (especially high-end carbon-reinforced): high stiffness and low toughness. The latter is caused by brittleness of the hard thermoset matrices and carbon fibres, and by stress concentrations at the fibres-matrix interface. When CNT/CNF are placed in the matrix or on the fibre surface, crack initiation and propagation in the matrix or on the interface are hindered thanks to several possible mechanisms. Some of these mechanisms have the same nature as in CNT/polymer composites (without fibres): cracks bridging by CNT/CNF, crack deflection, blunting of the crack tip, etc. [1]. Other mechanisms, related to the redistribution of stresses and changing of the stress concentration factors, are specific for the hierarchical mixture of nano- and micro-reinforcements [2].

Composites, which combine nano-reinforcements with conventional micro-meso hierarchy of FRC, are called by some authors "hybrid" or "hierarchical". The former term may be misleading in composites parlance, as "hybrid composite" normally means "composite combining different types of fibres" (i.e., glass/carbon hybrid). The latter term does not really distinguish the composites with nano-reinforcements, as any FRC has a hierarchy of the structure (micro (fibres)–meso (yarns or plies)–macro (part)) [3,4]. We will use a term "nano-engineered fibre reinforced composites" (nFRC) to designate the class of materials under consideration.

There are several ways to create nFRC. CNT, for example, can be

- dispersed in the matrix;
- dispersed in the sizing of the fibres, hence concentrating on the interface between the fibres and the matrix;
- introduced as a special ply in a laminate with CNT grown on a substrate;
- grown on the fibrous reinforcement (unidirectional or textiles), which creates a "forest" of CNT/CNF on the surface of the fibres (also called below "CNT/CNF-grown-on fibres/fabrics").

For the literature on the subject and an overview of the production methods of nFRC and their mechanical properties the reader is referred to the recent comprehensive reviews [5,6] of these

* Corresponding author. Tel.: +32 16 32 12 10; fax: +32 16 32 19 90.
E-mail address: Stepan.Lomov@mtm.kuleuven.be (S.V. Lomov).

0266-3538/$ - see front matter © 2010 Elsevier Ltd. All rights reserved.
doi:10.1016/j.compscitech.2010.11.024

methods. As shown in [5–8], the recent research has demonstrated that it is possible to achieve a significant increase in toughness after addition of CNT to fibre reinforced composite: such properties as fracture toughness G_{Ic}, interlaminar shear strength in nFRC are higher in comparison with FRC without nano-additions by a factor which may be as high as 3.

The last method in the list above, namely growth of CNT/CNF on the surface of the fibres, is the subject of the present paper.

This work originates from a simple observation in the lab. At one stage in the research CNT were grown on unidirectional (UD) carbon fibre plies from which prepregs were made and laminates were produced in an autoclave. The pressure used (about 1 bar) was enough for compaction of the laminate without CNT up to fibre volume fraction of 60%. However, when the same pressure was applied to the prepregs containing CNT-grown-on UD-plies, the volume fraction of the laminate was only 36%. The plate thickness increased almost twice. This indicated a drastic change of the compressibility of the fibrous plies after grafting them with CNT. This observation "triggered" the research effort described in this paper, which examines compression properties of dry fabrics with CNT/CNF grown on them.

The compressibility of a fibrous preform is defined as a dependency of the preform thickness h on the pressure p applied to its surface: $h = f(p)$. It is an important property as it largely affects preform processability and quality of a composite part. For composite manufacturing processes with a constant hydrostatic pressure applied to the reinforcement (such as vacuum infusion, light RTM, autoclave), the compressibility will largely define the fibre volume fraction in the composite part. This is because the thickness directly defines the fibre volume fraction V_f by an equation $V_f(p) = (m/\rho)/h(p)$, where m is the areal density of the preform, ρ is the physical density of the fibres. If the preform is not compressible enough, the economical vacuum infusion process cannot be used to produce parts with a sufficiently high fibre volume fraction. This is because the pressure is limited by 1 bar (0.1 MPa), as a flexible vacuum upper bag/mould on rigid lower mould is used. In the RTM process, with two rigid moulds on both sides of the preform, the compressibility of the latter defines the force needed for closing the mould. In RTM processes with one semi-deformable (rubber or composite) mould the resistance of the preform to compression defines the deformation of the rubber part of the mould and hence the precision of the final part thickness.

The compressibility of fibrous assemblies in general (fabrics, non-wovens, bulk fibres like wool) and of composite reinforcements in particular is well understood. The reader is referred to [9–13] and the bibliography in these papers for a deeper insight in the mechanical phenomena, measurement methods and models of the compression of composite preforms. The compressibility is controlled by such parameters of the preform structure and fibre properties as bending rigidity of the fibres, their waviness (crimp), tightness of the yarn packing, defined by the yarn twist, inter-yarn and inter-fibre porosity, presence of sizing. A typical pressure vs thickness diagram is shown in Fig. 1. The figure shows three successive cycles of compression of the same sample. For each cycle, region I of the diagram (low pressure) is controlled by change of the fibre crimp, and the low compression resistance is given by low bending resistance of the fibres. Region II is intermediate. In the high pressure region III the fibres come close together, the number of contacts of between them increases dramatically, there is no more freedom for the fibres to bend, and the resistance to compression is more and more defined by high Hertzian contact forces rather than by bending of the fibres. Fibres (glass, carbon, aramid, etc.) themselves can be considered as not compressible in the range of pressure used in composite manufacturing. Hence there exists a limit for the compaction [11,14] – a horizontal asymptote for the pressure-thickness diagram. If the compaction

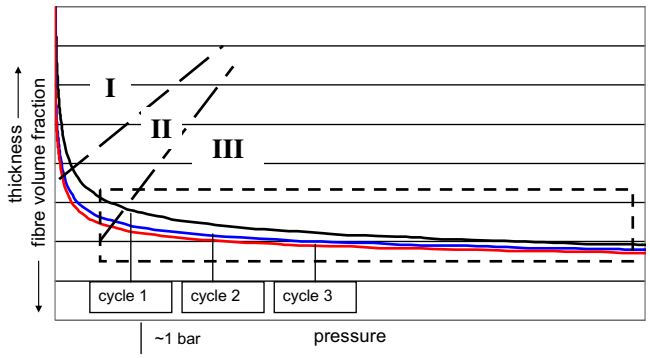

Fig. 1. Typical compression diagram of a fibrous preform. The dashed rectangle indicates a practical range of the thickness and pressure for composite processing.

load is released and then applied again in a second, third, etc. cycle, then a certain part of the deformation is not recovered when the load is released, and the thickness under given load decreases for each successive cycle. Typically after the third cycle the differences between the subsequent cycles become negligible. For typical composite preforms the practically interesting region of the final state of the preform on the compression diagram is shown in Fig. 1 by the rectangle. It corresponds to a fibre volume fraction of 50–60%. To reach this range, a typical preform has to be compacted into regions II–III of the diagram, with pressure from the vacuum range (0.8–1.0 bar) up to several bars.

As the regions II–III correspond to quite tight packing of the fibres, it is no surprise that growth of CNT/CNF on the fibre surface can affect the conditions of this packing. The questions, which we address in this paper, are:

- Does coverage of fibres with CNT/CNF change significantly the compaction resistance of a typical composite preform?
- Should the change of compaction behaviour of CNT/CNF-grown-on preform be taken into account during manufacturing of nFRC?

For this exploratory study, common and widely used woven carbon fibre reinforcements were selected as baseline materials. CNT/CNF were grown on the fibres using a Chemical Vapour Deposition (CVD) method with catalyst particles distributed on the fibres. No attempt was made in this study to optimise growth parameters and processing conditions, such as catalyst distribution on the fibres, weight fraction of the CNT/CNF, etc. We also leave aside extremely important problems of possible deterioration of properties of the carbon fibres due to the interaction with the catalyst. Our aim is to determine, whether CNT/CNF-growth poses any problem for composite manufacturing and to estimate the seriousness of the above problems, rather than to find optimised solutions for the growth.

According to the authors' knowledge, these questions, in spite of the obvious practical importance, were never addressed before. They stay in line with other aspects of processing of nFRC, which are starting being addressed in the literature [15]. If CNT/CNF-growth on fibrous preforms is destined to leave the laboratories and enter composites production facilities, they have to be answered and, if answered in the affirmative way (as it will be shown in the paper), have to be followed by research programs for optimisation of the current FRC-processing technologies for new nFRC.

2. Materials and the CNT/CNF growth process

Parameters of the fabrics, chosen as the baseline materials and a substrate for growth of CNT/CNF, are shown in Table 1. Fig. 2 depicts the surface view of them. The fabrics were processed in

Table 1
Parameters of the carbon woven fabrics.

Fabric ID	A	B
Producer	TenCate	Porcher industries
Weave	5H satin	Plain
Warp/weft yarns	3K Torayca® T300J	3K HS
Ends/picks count (yarns/cm)	6.4/6.4	5.0/5.0
Areal density (g/m^2)	280	200
Fibre diameter (μm)	7	7
Presence of sizing	No, de-sized at manufacturer prior to delivery	Yes

Table 2
Parameters of the CVD processes.

Lab	University of Twente	Nanocyl
Fabric ID	A	B
Dimensions of the fabric sample	26 × 31 cm	4 × 25 cm
Deposition of catalyst precursor		
Catalyst precursor	Nickel nitrate	Iron + cobalt salts
Catalyst solvent	Acetone	Water + ethanol
Temperature of the impregnation	25 °C	RT[a]
Drying time	10 min	12 h
Drying temperature	RT	RT
Drying conditions	Air	Air
Heating up to the reaction temperature (inert)		
Temperature	600 °C	750 °C
Time	90 min	45 min
Gas	Nitrogen	Nitrogen
Flow rate	2 l/h	2 l/h
Reduction of metal salts		
Temperature	600 °C	n/a
Time	60–90 min	n/a
Gases	N_2:H2, ratio 70:30	n/a
Flow rate	0.666 l/h	n/a
CNT/CNF growth		
Temperature	600 °C	750 °C
Time[b]	AG: 37 min	BG1: 10 min; BG2: 15 min
Gases	N_2:C_2H_4:H_2 (50:40:10)	N_2:C_2H_4:H_2 (50:40:10)
Flow rate	2 l/h	4 l/min

[a] RT: room temperature.
[b] The times shown correspond to the samples AG, BG an BG2 (see Table 3); one can vary the growth time according to the desired amount of the growth.

two laboratories: University of Twente (fabric A) and company Nanocyl (fabric B). The fabrics are different by the weave style, but have not-that-different ends/pick count and areal density. Fibres in fabric A have no sizing (de-sized at manufacturer's), fibres in fabric B are sized. Table 2 summarises parameters of the CVD process used in the two labs.

The size of the substrate used for growth of CNT/CNF (shown in Table 2) is limited by the dimensions of the reactors in the labs.

CNT/CNF were grown using the following steps:

1. Deposition of the catalyst precursor: the fabric is immersed in a solvent containing the catalyst precursor and is dried afterwards at room temperature in open air.
2. The sample is then heated up to the temperature used in the growth process in an inert atmosphere
3. For fabric A the metal salts on the fabric are reduced into pure catalytic metal particles (hydrogenation of nickel nitrate to elementary nickel); for fabric B this step is omitted, as in preparation of this test series Nanocyl has tried growth with and without a reduction step and no differences were observed in the quality or yield of the growth. During the steps 2 and 3 the sizing on the carbon fibres should be burned out.
4. CNT/CNF growth: the fabric is processed in the gas chamber with N2:C2H4:H2 (proportion 50:40:10) for the time chosen to achieve the desired yield of the growth.

Catalysts, gases used in the different steps, duration and temperature of the processing are shown in Table 2, for the two processes adopted in the two labs.

Table 3 summarises parameters of the samples which were tested in compression. At the University of Twente samples with one CNT/CNF growth loading level has been produced, using fabric A. This material is labelled AG. In Nanocyl two types of samples were produced (using fabric B), with lower and higher growth loading. These samples are referred to as BG1 and BG2. Apart from production of the grown-on samples, the fabrics were also tested for compressibility after they were only subjected to catalyst deposition and thermal treatment at the temperature of the growth step, without N_2:C_2H_4:H_2 gas flow (these samples are referred to as AC and BC). Table 3 shows dimensions and a number of fabric samples for each group, the change of mass of the fabric during the growth process.

The data in Table 3 show that addition of Ni catalyst (fabric A) increases the sample mass by 0.5%. This corresponds well to the fact that there is no sizing on the fibres to be burned away. The negligible change of the fabric mass after catalyst deposition was confirmed by TGA analysis. When Fe catalyst treatment is used for fabric B (see Table 3) the sample mass has decreased by 7.7%

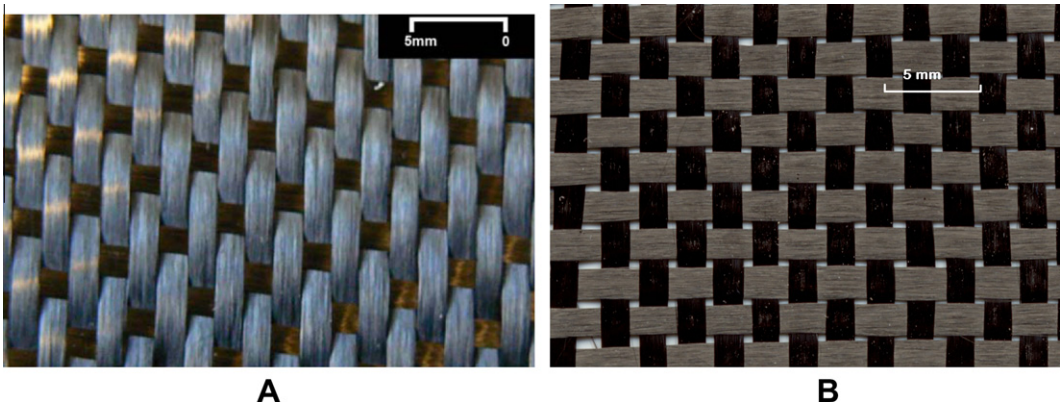

Fig. 2. Scanned surfaces of the fabrics A and B.

Table 3
Fabric samples used for compression tests.

Lab	University of Twente	Nanocyl	
Fabric ID	A	B	
Fabric samples catalyst treated only – sample ID	AC	BC	
Number of samples	1	5	
Relative mass, % (the mass of virgin fabric = 100%)	100.5	92.3 ± 0.3	
Fabric samples with CNT/CNF growth – sample ID	AG	BG1	BG2
Number of samples	1	5	5
Relative mass, % (the mass of virgin fabric = 100%)	106.5	105.9 ± 1.4	110.6 ± 0.3

Note: "±" means standard deviation.

against the mass of the virgin fabric. This can be partially explained by burning away the sizing.

Fig. 3 shows catalyst particles on fibres after the treatment. The size of the particles varies from 20 to 150 nm (fabric A) and from 5 to 10 nm (fabric B). After CNT/CNF growth, the mass of the samples increases by 6.5% (sample AG), 5.9% (BG1) and 10.6% (BG2) in relation to the mass of the virgin fabric. However, if the change of mass after catalyst treatment is taken into account, then the mass of the growth in relation to the mass of the fibres without sizing is 6.0% (AG), 14% (BG1) and 18% (BG2). The grown CNT/CNF were inspected under SEM and TEM. A piece of fabric with the width of about 1 cm was cut out, and a yarn was carefully taken from this strip and placed under SEM. Because of this handling, one cannot exclude certain loss of the grown CNT/CNF from the surface of the fibres. For TEM observations the grown CNT/CNF were mechanically removed from the fibres and inspected under TEM.

Figs. 4 and 5 show SEM and TEM images of samples AG. One observes quite even distribution of the growth over surface of the fibres (Fig. 4A) and absence of amorphous carbon phase. The catalyst particles can be seen on the ends of CNF. Higher magnification SEM images (Fig. 4B and C) and TEM (Fig. 5) show that the growth consists of CNF, probably with cup-type morphology, of different diameters: thin ones, with diameter in the range 20–50 nm, and very thick CNF with diameter about 200 nm. The CNF are organised in a dendrite-like structure covering the carbon fibres.

Figs. 6 and 7 show SEM and TEM images of samples BG1/2. On the samples BG1 one notices not-so-even coverage of the carbon fibres surface and strong diameter distribution of the CNT/CNF (Fig. 6A). The BG1 samples exhibit a considerable non-homogeneity in the growth yield: the standard deviation of the mass of the grown-on samples is 1.4%, with the average growth loading of 5.9% in comparison with the virgin fabric (Table 2), and the range of the mass increase from 4.3% to 7.6%. Fig. 6B shows SEM images of samples BG2. There is a good reproducibility of growth yield for these samples: the standard deviation is 0.3%, with the average mass increase of 10.6% (Table 2) and the range of the mass increase from 10.3% to 11.0%. There is a rather good homogeneity of coverage of the fibres. Two populations of CNT/CNF are present (Fig. 7). On the surface of the fibres CNT with diameter about 20 nm are observed. The tubular structure of the CNT is clearly seen in TEM images of Fig. 7. In the inter-space between the carbon fibres cup-type CNF are seen with diameter 50–100 nm.

3. Measurement method

Compression tests were done on a displacement-controlled testing machine Instron 4467 with a load cell of 1 kN. The test

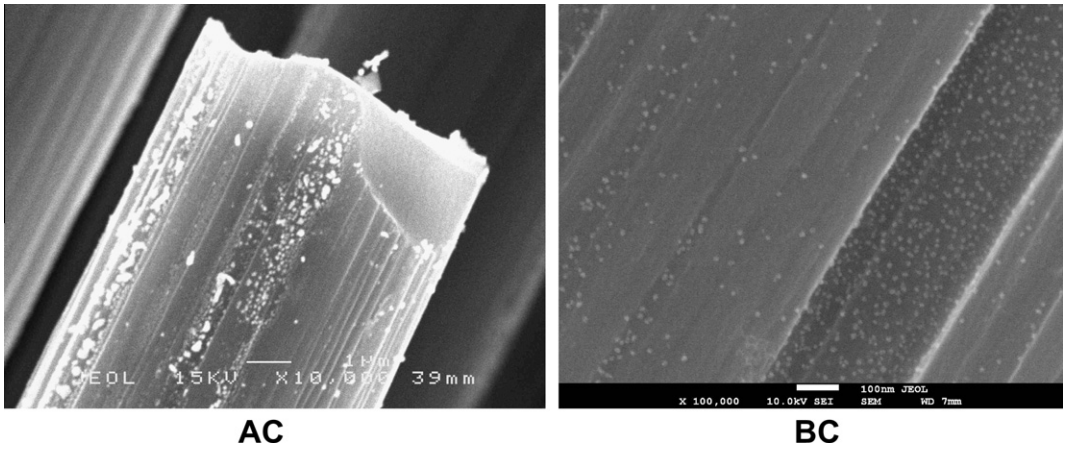

Fig. 3. SEM images of carbon fibres after catalyst treatment, samples AC and BC.

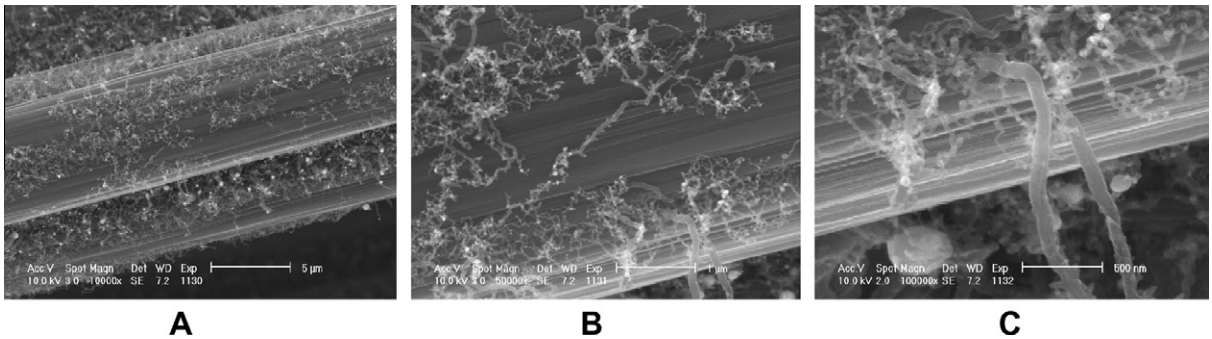

Fig. 4. SEM images of carbon fibres with CNF growth, samples AG: (A) distribution of the CNF over the fibre surface; (B, C) two types of CNF.

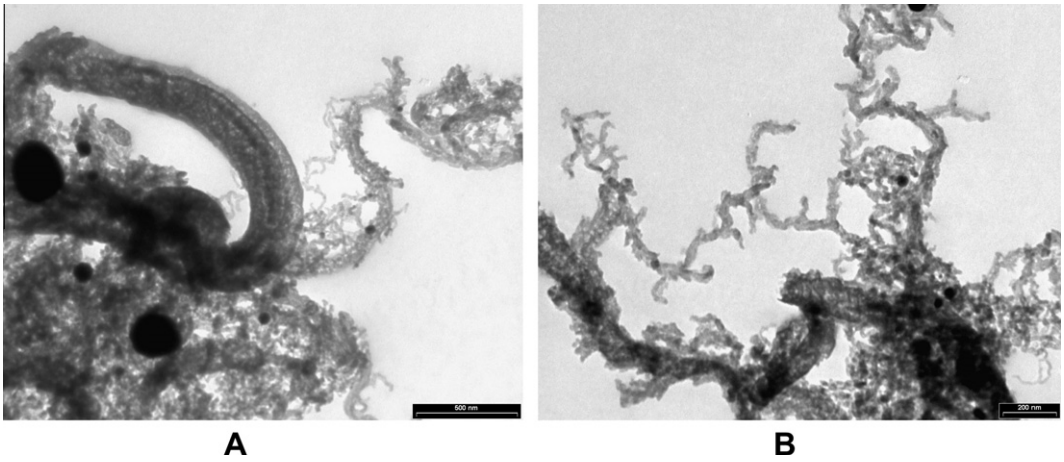

Fig. 5. TEM images of CNF growth, samples AG: (A) a thick CNF; (B) thinner CNF with dendrite organisation.

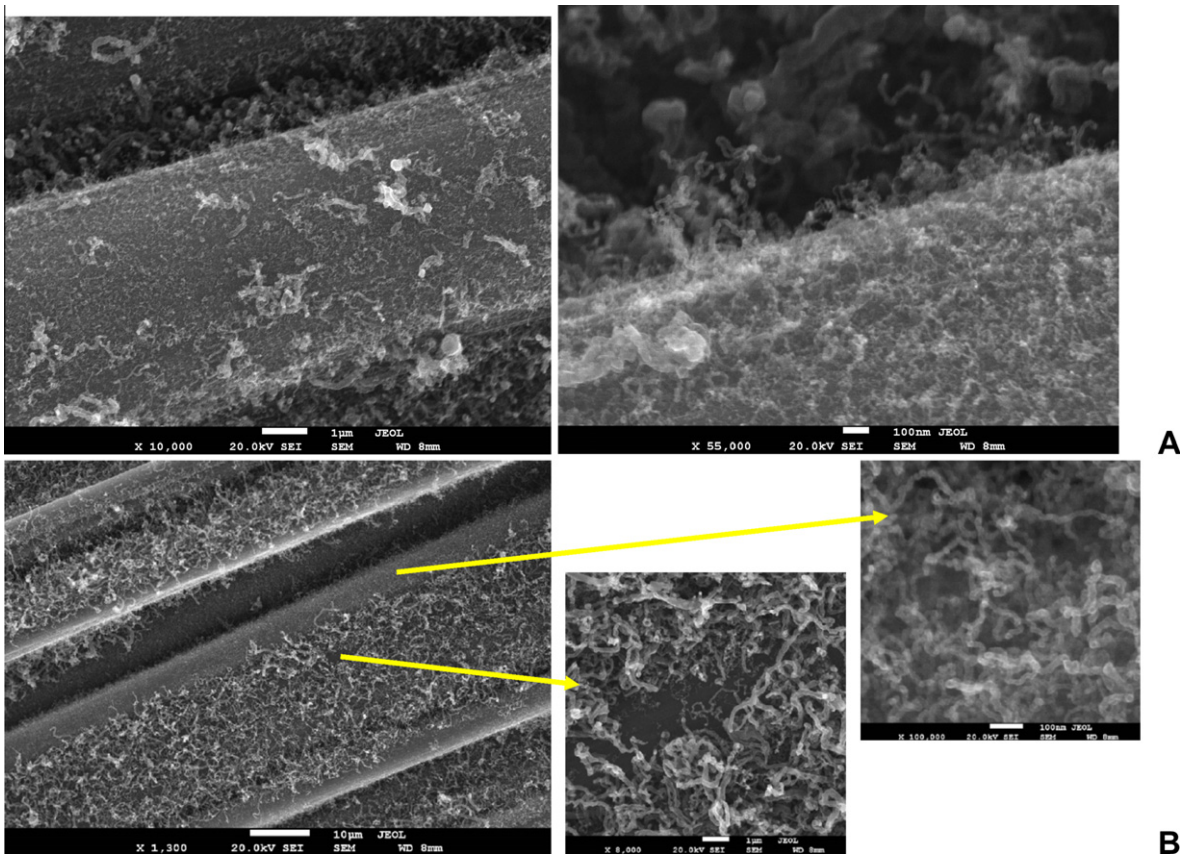

Fig. 6. SEM image of carbon fibres with CNT/CNF growth, samples BG1 (A) and BG2 (B).

speed was 1 mm/min. Fig. 8 illustrates the measurement technique. A self-aligning compression rig with a ball-pivot bottom platform (Fig. 8A) was used. When the first test is done without the sample, the platform aligns itself with the upper plate, fixed in the moving crosshead of the machine. After that, three tests are done without a specimen, to establish a calibration curve (Fig. 8B), which allows calculating the compressed sample thickness h under the load F, accounting to the compliance of the rig: $h(F) = X(F) - X_0(F)$, where $X(F)$ and $X_0(F)$ are the displacement, corresponding to force F in the tests with the sample and without it. The standard deviation of the calibration curve $X_0(F)$ is in the range of 0.0015–0.0017 mm for the whole range of the applied force (maximum 900 N). This is about 1.5–1.7% in relation to the total displacement of the compression platform under this force in the calibration test (0.10 mm).

The tests were done on one and four layers of the fabric, which allows estimating the nesting effect [13]. In the case of four-layer specimens the plies were oriented in the same way (coinciding warp directions). Three successive cycles of compression were performed to measure the compressibility in the relaxed and the "set" state of the preform [12,16]. The diameter of the round upper plate and the compression platform is 70 mm, which is more than the width of the fabric B strips (samples BC, BG1, BG2). This does not apply to fabric A samples. However, for the both fabrics the specimens with approximate dimensions 40×40 mm were cut out and put in the compression device.

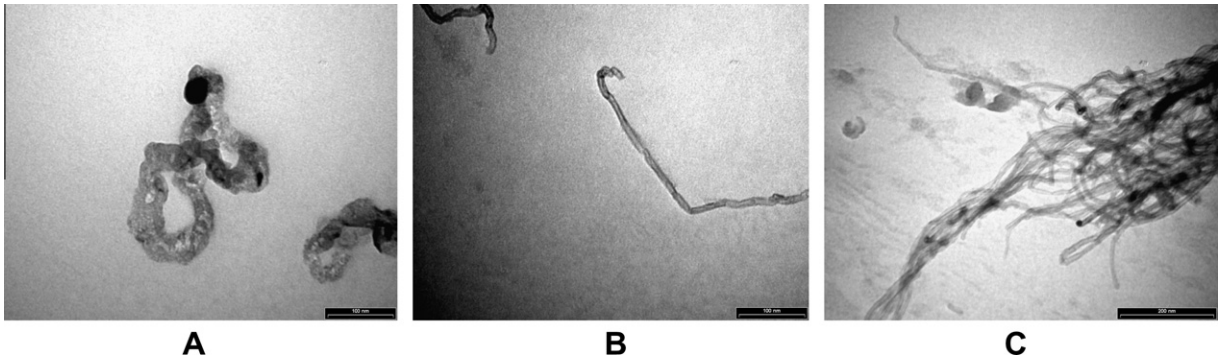

Fig. 7. TEM images of CNF growth, samples BG: (A) CNF; (B, C) CNT.

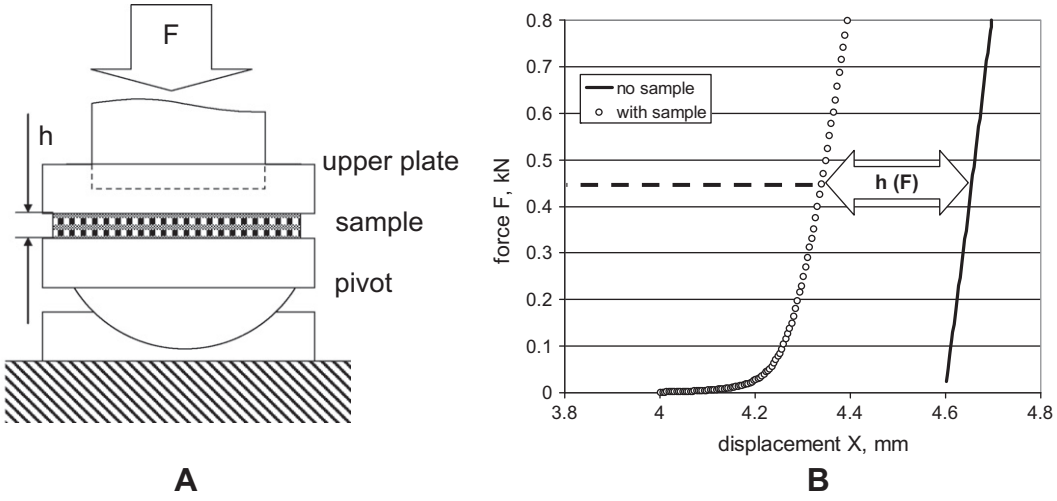

Fig. 8. Measurement technique: (A) scheme of the compression rig; below: sample strip and the compression plate; (B) data processing.

The dimensions of the fabric specimens are measured with a considerable error because of difficulties of straight cutting of a non-stable fabric. When a four-ply specimen is prepared, the sizes of the plies in the stack are somewhat different. The minimum ply dimensions in the stack of four plies were taken for the processing in this case. To assess the acceptability of the measurements on the small specimens in comparison with the larger sample, the diagrams $p(h)$, obtained from measurements on 40×40 mm specimens of the virgin fabric A, were compared with the pressure vs thickness diagrams, measured in the centre of square samples of the same fabric with dimensions 150×150 mm. The difference of the thickness of the fabric at the same pressure was about 0.005 mm, whilst the standard deviation of the thickness in both test types was in the range 0.005–0.01 mm, with at least three tests for every type of the sample. Therefore the measurements on the 40×40 mm specimens were accepted as valid and all the data quoted below are obtained on these specimens using the test and the data processing procedure depicted in this section.

The load limit of 0.9 kN (safety of the load cell) gives a maximum pressure on the specimen of about 0.5 MPa. Compression behaviour of CNT/CNF-grown-on reinforcements for higher loads will be a subject of future work.

4. Compression diagrams

For each of the fabric samples (A, AC, AG; B, BC, BG1, BG2 with one and four plies – 14 variants in total) compression tests were done on three specimens (42 tests in total) with three consecutive cycles of compression in each test. Figs. 9 and 10 give an overview of all the compression measurements. All the data in these figures and elsewhere in the paper are presented in terms of thickness of one ply, which is directly measured for the case of one-ply specimen, or is the total thickness of a four-plies specimen divided by four. One out of three tests was selected for presentation in Figs. 9 and 10 – namely, the test, for which the thickness of one ply at pressure 0.1 MPa is the closest to the average thickness in the three tests.

4.1. Different compression cycles

Analysis of the graphs presented in Figs. 9 and 10 shows that the compression behaviour of all the tested fabric variants, including the grown-on samples, follows the pattern typical for textile preforms as schematically shown in Fig. 1: the fabric is "set" after the second cycle, and the difference in thickness of the fabric at a given pressure between the third and the second cycle is much less than between the second and the first cycle. This behaviour is typically observed in studies of compressibility of textile preforms [9,10,12,13]. Following the practice in these studies the second compressive cycle is taken as characteristic for the fabric compression resistance.

4.2. Variability and repeatability of compression diagrams

The measurements have shown a remarkable repeatability of the compression behaviour of all the variants of samples. The

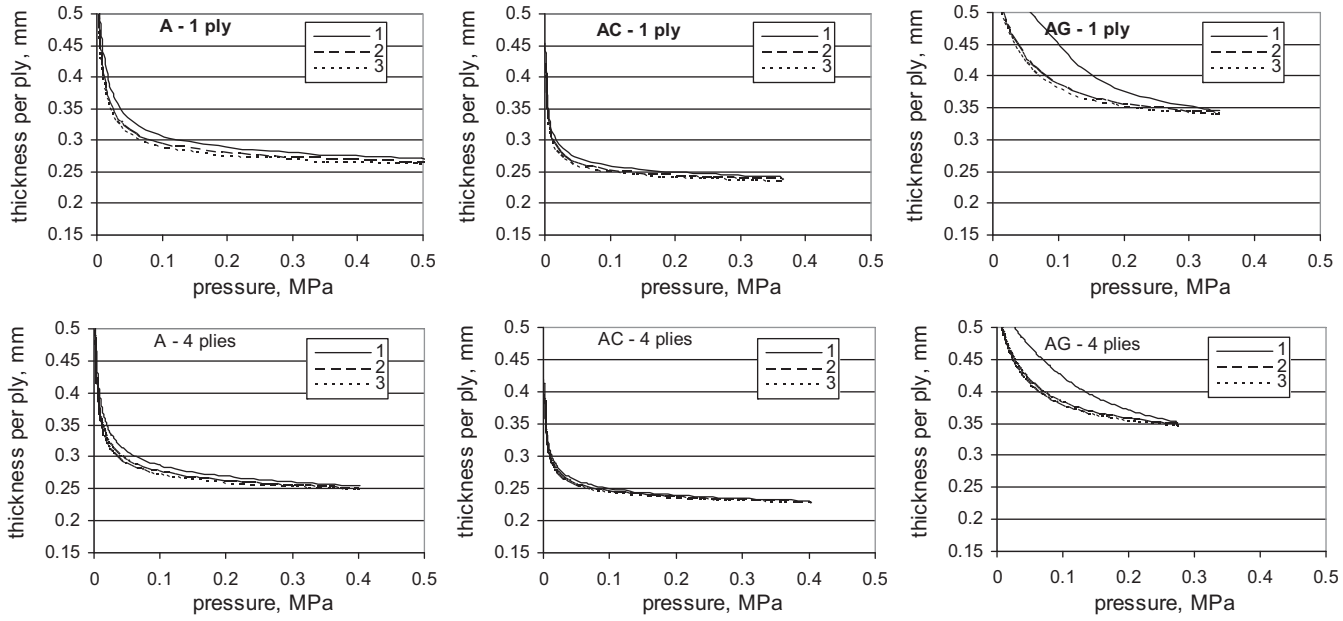

Fig. 9. Compression diagrams – fabric A. Representative samples, three successive compression cycles (designated by numbers in the graph legends). See Table 3 for abbreviations of the sample types.

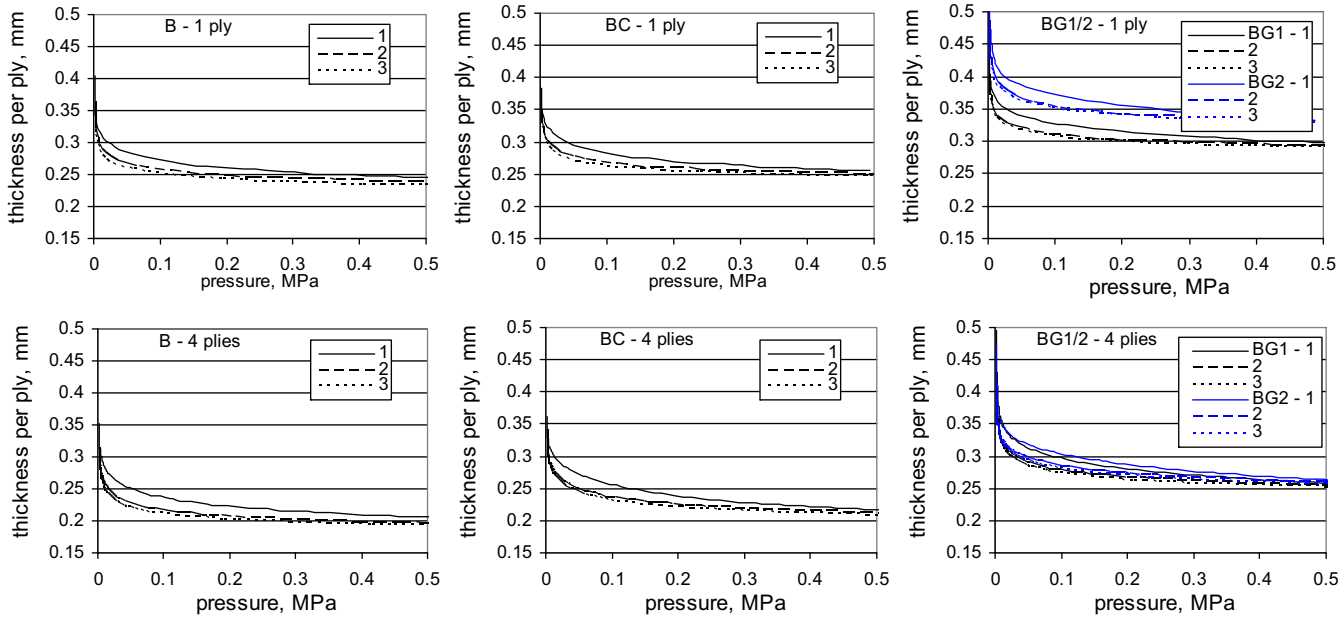

Fig. 10. Compression diagrams – fabric B. Representative samples, three successive compression cycles (designated by numbers in the graph legends). See Table 3 for abbreviations of the sample types.

low variability of the specimen thickness under a given pressure is illustrated in Table 4, which gives the thickness of one ply of fabric samples under pressure 0.1 MPa (1 bar) for all the tested samples. This characteristic will be shortly called in the rest of the paper "1 bar ply thickness". The coefficient of variation (CV) of 1 bar ply thickness for all the samples is below 5%, and for majority of the samples is about 3% or less.

Fig. 11 shows plots of fibre volume fraction in the sample vs applied pressure for the second compression cycle of all the specimens (three of each kind) of virgin, catalyst treated and grown-on samples, allowing to assess the variability of the data for all the range of pressure in the test. The fibre volume fraction is calculated as $V_f = m \cdot N/(t(N,p) \cdot \rho)$, where $t(N,p)$ is the thickness of N plies under pressure p, m is the areal density of the fabric, given in Table 1, and $\rho = 1.78$ g/cm^3 is density of carbon. It can be seen that the variability of the sample thickness over the whole pressure range follows the same trend as 1 bar ply thickness given in Table 4 as discussed above.

The measured variability of the sample thickness under given pressure corresponds to the behaviour typically observed for textile preforms [9,10,12,13]. This gives credibility to the measurement technique used here and allows proceeding to the analysis of changes in the compression behaviour caused by CNT/CNF growth.

Table 4
Thickness of one ply of fabric samples under pressure of 0.1 MPa, the second compression cycle.

Number of plies (N)	Sample	Variability, 3 tests			Nesting		De-sizing and catalyst effect[a]		Effect of growth[a]	
		Average thickness $t(N, 0.1\ \text{MPa})/N$ (mm)	Standard deviation (mm)	Coefficient of variation (%)	Thickness difference $t(4, 0.1\ \text{MPa})/4 - t(1, 0.1\ \text{MPa})$ (mm)	Nesting coefficient $k_{nest}(N, 0.1\ \text{MPa})$ (%)	Thickness change (mm)	Relative thickness change (%)	Thickness change (mm)	Relative thickness change (%)
1	A	0.291	0.003	1.0			0	0		
	AC	0.252	0.001	0.4			−0.040	−13.6		
	AG	0.399	0.019	4.7					0.107	36.9
4	A	0.276	0.005	1.7	−0.015	−5.2	0	0		
	AC	0.244	0.001	0.6	−0.007	−2.9	−0.032	−11.5		
	AG	0.381	0.005	1.3	−0.018	−4.5			0.105	37.9
1	B	0.258	0.001	0.2						
	BC	0.267	0.001	0.5			0.009	3.4		
	BG1	0.314	0.003	0.8					0.056	21.7
	BG2	0.343	0.017	4.9					0.084	32.7
4	B	0.216	0.007	3.3	−0.042	−16.2				
	BC	0.238	0.007	2.8	−0.029	−10.7	0.022	10.1		
	BG1	0.284	0.006	2.0	−0.030	−9.6			0.068	31.3
	BG2	0.297	0.010	3.3	−0.046	−13.4			0.080	37.1

[a] In comparison with the virgin samples of the same fabric (A or B samples) and the same number of plies.

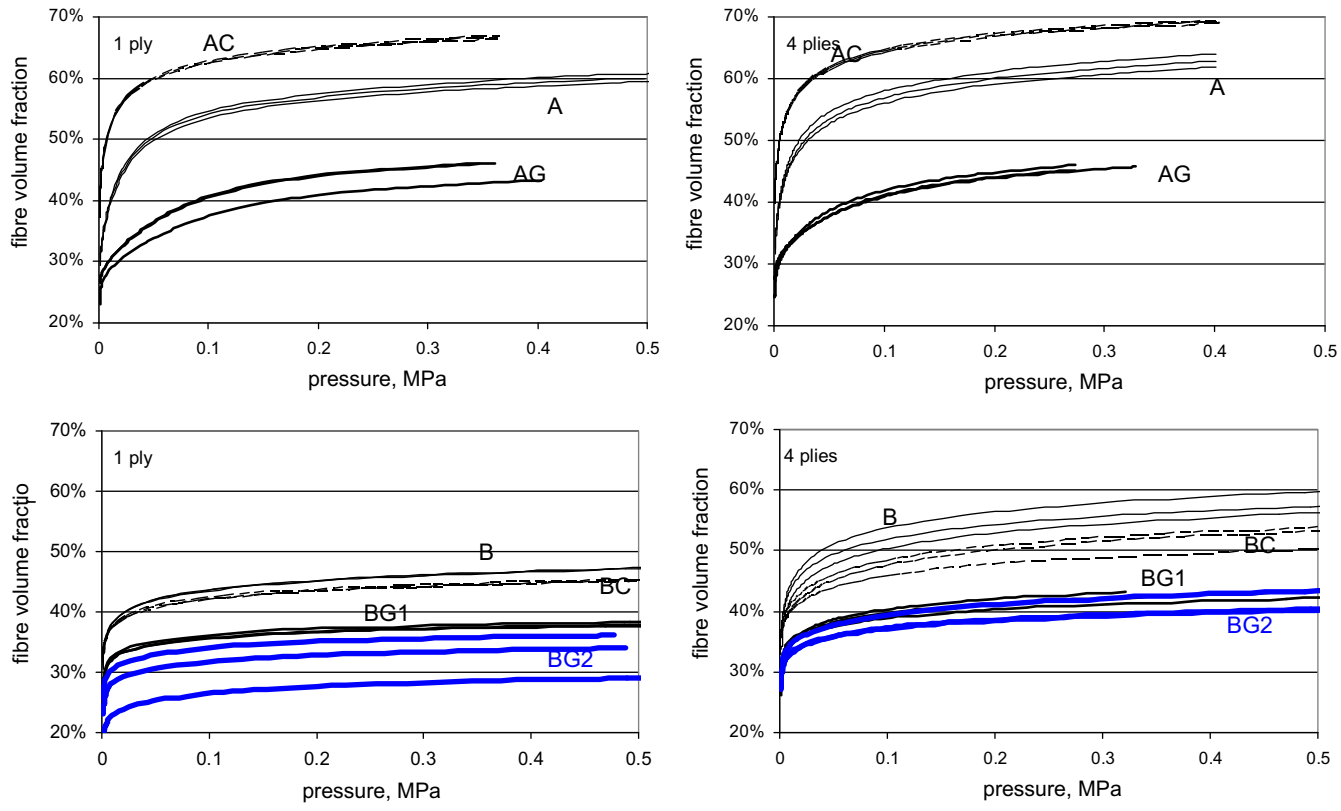

Fig. 11. Fibre volume fraction in the tested samples vs applied pressure.

4.3. Nesting

Nesting of plies of a multi-layer textile preform is an important phenomenon, affecting the thickness of the preform and hence the fibre volume fraction in the composite [13]. The fabric has a certain surface relief and the layers of the fabric are positioned one in relation to another in a random manner. When the layers are compressed together, the "hills" and "valleys" of two adjacent layers "nest" one into another. The total thickness $t(N)$ of N layers becomes less than the $N \cdot t(1)$, where $t(1)$ is the thickness of one separate layer. The reader is referred to [13,17,18] for a detailed analysis of the geometrical aspects of the nesting effect in woven, braided and non-crimp fabric laminates. Nesting naturally affects the compression behaviour of textile preforms, resulting in decrease of the average thickness of one ply of multi-layered preform for a given pressure in comparison with the thickness of one ply of the same preform at the same pressure [12,13,16,19–25]. The same effect can be expressed as an increase of the fibre volume fraction of laminate, compacted under a given pressure, with increasing number of layers of the laminate. Nesting of the layers in a

laminate affects such properties of the composite as permeability [26], compression strength [27], damage initiation and progression [28–30].

Nesting can be characterised by the nesting coefficient, defined as

$$k_{nest}(N,p) = \frac{t(N,p)/N - t(1,p)}{t(1,p)}.$$

Table 4 shows the difference of the 1 bar ply thickness between 4-ply and 1-ply laminates and the nesting coefficients $k_{nest}(4, 0.1\ \text{MPa})$ for all the measured samples. The values of the nesting coefficients $k_{nest}(4,p)$ for the full pressure range from $p = 0.02$ to $p = 0.5$ MPa do not differ from the values $k_{nest}(4, 0.1\ \text{MPa})$ by more than 1%.

Two conclusions can be drawn from analysis of the values given in Table 4. First, fabric A (5-harness satin) exhibits much lower nesting than fabric B (plain weave), for virgin and grown-on fabrics, as well as for the fabrics in the intermediate stages of the growth processing: the nesting coefficients for the fabric A are in the range from 2.9% to 5.2%, for the fabric B in the range from 0.6% to 16.2%. This difference is explained by the lower roughness of the surface of the satin fabric (A) in comparison with the plain weave (B). The qualitative difference and the actual values of the nesting coefficients are in agreement with the published theoretical analysis and experimental observations for plain weave and satin woven fabrics [13,19,20]. Second, there is no significant change of the nesting coefficients as a result of the growth. This underlines the fact that CNT/CNF growth is a micro-level, inter-fibre, intra-yarn process, whilst the nesting is a meso-level, inter-yarn and inter-ply effect. We have reported elsewhere [31,32] that the permeability of fabric A has not changed after the growth (in laminates with the same fibre volume fraction), which is in accordance with the small change in nesting shown here.

4.4. Change of compressibility due to adding the catalyst

Addition of the catalyst, which precedes the growth of CNT/CNF, changes the compressibility of the fabric to a certain extent. This change is different for the two studied fabrics and used processes.

Fabric A becomes softer after adding the catalyst and temperature treatment. The softness is felt by touch; the individual carbon fibres in yarns become loose. This change leads to better compressibility of the samples AC: the 1 bar ply thickness is decreased by 13.6%/11.5% after adding the catalyst (Table 4, 1 ply/4 plies); the same change of thickness is seen over all the range of pressures (Fig. 11).

The easier compressibility of fabric A after catalyst treatment may be linked to the phenomena studied in [33–37], namely to deterioration of the properties of the fibres due to a partial 'dissolution' of the carbon of the cloth within the activated metallic phase, or to a change in the morphology of carbon fibres at atomic level that comes from the reconstruction of the graphitic structure during heat treatment, even if there is no catalytic gasification of the fibres as the mass loss after treatment is negligible. The investigation of this problem needs further research and is out of scope of the present work. To discuss what is exactly at the origin of this phenomenon is not the point of this publication and should require more detailed experiments. Moreover, the higher compressibility of the catalyst-treated samples highlights the loss of compressibility after the subsequent CNF growth.

Contrary to fabric A, fabric B becomes more rigid after addition of the catalyst, and its compressibility becomes worse: the 1 bar ply thickness of samples BC is increased by 3.4%/10.1% (Table 4, 1 ply/4 plies). The same change of thickness is seen over the whole range of pressures (Fig. 11).

The relatively small decrease of compressibility, seen in fabric B, can be in principle caused by a certain "gluing" together of the carbon fibres by residuals of the catalyst precursor. However, no evidence of this was seen in SEM observations. This should be a subject of future research. In any case, the stiffening effect of the catalyst for fabric B is much less than the effect of CNT/CNF growth, discussed in the next section.

4.5. Change of compressibility due to CNT/CNF growth

After the preliminary considerations in the previous sections the main effect on the preform compressibility, namely the one of the CNT/CNF growth, can be discussed. The compressibility is significantly deteriorated after the growth. Table 4 shows the change of 1 bar ply thickness for the sample AG: 36.9%/37.9% (1ply/4 plies) – in comparison with the virgin fabric A. When the sample AG is compared with the sample AC (which became more compressible after thermal treatment and addition of the catalyst), the change of the 1 bar ply thickness becomes 58.3%/56.1%. The same change for the fabric BG1 is: 21.7%/31.3% (BG1 vs B) and 17.6%/19.3% (BG1 vs BC); for the fabric BG2: 32.7%/37.1% (BG2 vs B) and 28.4%/24.7% (BG2 vs BC). In view of the low scatter of the thickness values (below 5%) these changes are statistically significant; the analysis of variations shows a confidence level of the difference of 0.99 or more.

The same deterioration of compressibility after the growth happens over the whole range of pressures in the compression tests. Fig. 11, which expresses the compressibility in terms of the sample fibre volume fraction, shows that the grown-on samples are compressed poorly over the studied range of pressure and the change of compressibility is close to the characteristics discussed above for 1 bar ply thickness. Analysis of the data of Table 4 and Fig. 11 leads to several interesting observations.

- A given number of layers of fabric B provides a lower fibre volume fraction for a given pressure than the same number of layers of fabric A, and this relation holds also for grown-on fabrics.
- The change of compressibility of fabric A after CNT/CNF growth is higher than that of the fabric B (samples AG and BG1 are compared, which have close increase of the sample mass after growth). This allows concluding that the CNT/CNF growth on fabric A is more resistant to compression than the one on fabric B. It may be related to the different nature of the growth. Growth in samples AG consists of CNF with diameter 10–50 nm and thick CNF with diameter of about 200 nm. Growth in samples BG1/BG2 consists of CNT with diameter 10 nm and CNF with diameter 50–100 nm. This means that the CNT/CNF growth in samples BG1/BG2 in average have bending rigidity lower than in samples AG, hence the compressibility of the former is better. This explanation is in accordance with theories of resistance of random assemblies of CNT in [38,39].
- Growth yield (compare the curves for samples BG1, with yield of 6% and BG2, with yield of 11%) has more pronounced effect for 1 ply samples, where the change of the fibre volume fraction is approximately proportional to the change of the sample mass. In 4 plies samples increase of the growth yield does not bring a pronounced increase of the change of fibre volume fraction.
- The changes of compressibility due to the CNT/CNF growth bring dramatic changes in processability of the fabrics. Consider 4 plies samples of fabric B. The fibre volume fraction of samples B at pressure 0.1 MPa (vacuum infusion) is 52%. For the grown-on samples BG1 and BG2 the fibre volume fraction under the same pressure is 38%...40%. Even at pressure 0.5 MPa (autoclave/RTM range) the fibre volume fraction of the grown-on samples does not exceed 42%.

5. Discussion

The observed poor compressibility of CNT/CNF-grown-on preforms can have important consequences for the choice of the manufacturing process of nFRC and the processing window of this process. The need of high pressures can be prohibitive for the use of economical vacuum assisted processes. Once the problem is clearly demonstrated, optimisation of the CNT/CNF growth from the point of view of composite manufacturing can be addressed.

Explanation of the high compression resistance of CNT/CNF-grown-on preforms should start from the observation made when the nesting effect was discussed: the unchanged nesting behaviour of the grown-on preforms suggests that the increased resistance is a micro-level effect and is related to the compressibility of the CNT/CNF "forest". The latter can be seen as an assembly of randomly distributed slender elastic "fibres". The theory of compressibility of such an assembly is well developed for non-woven textiles, and can be applied to the "forest". The present authors [39] and others [38] have done the preliminary theory development on these lines, and have shown that a CNT "forest" can indeed develop very high compression resistance due to very high number of contacts in the assembly. This direction of research will be continued in future work. An important component of the future research should be more detailed experimental studies of compressibility of yarns with CNT/CNF growth on one hand (to eliminate meso-scale effects like nesting present when a fabric is compressed) and, on the other hand, of CNT/CNF forests on the sub-micron level.

The same observation of the unchanged nesting effects suggests that the compressibility of a reinforcement will also decrease as a result of CNT/CNT growth in the case of other preform architectures, for example, textile or UD laminates with different orientation of the plies, or made by individual filament/tape laying process (as winding). This will be made more clear in the future work on compressibility of, on one hand, yarns, and on another hand, other types of textile preforms with CNT/CNF growth.

6. Conclusions

The compressibility of carbon woven reinforcements is seriously affected by the growth of CNT/CNF on the surface of the fibres. The fibre volume fraction, achievable by compaction under pressure of 0.1 MPa (1 bar), is decreased from 65% for the baseline fabric A to 41% for CNT/CNF-grown-on fabric AG, and from 52% for the baseline fabric B to 40% for CNT/CNF-grown-on fabric BG1 (data for compaction of four plies, second compaction cycle, growth yield 6 wt%). The change of compaction behaviour of a CNT/CNF-grown-on preform should be taken into account during manufacturing of nano-engineered FRC. New research is needed to optimise the current FRC-processing technologies for new nano-engineered composites.

Acknowledgements

The work in K.U. Leuven was done within GOA/10/004 project "New model-based concepts for nano-engineered polymer composites", funded by the Research Council of K.U. Leuven. The collaboration between K.U. Leuven and Nanocyl S.A was performed under the framework agreement between the Department MTM, K.U. Leuven and Nanocyl S.A. The work in the University of Twente is done within Transforce ("Transverse Reinforcement of Carbon Fibre Composites with Carbon Nano Fibres") project primary funded by STW, The Netherlands. The research visit of Dr. M. Karahan to K.U. Leuven has been funded by a Tubitak scholarship (program BIDEB 2219, Turkey) and supported by K.U. Leuven. The help of Bart Pelgrims, Kris Van de Staey and Rudi De Vos (Department MTM, K.U. Leuven) is gratefully acknowledged.

References

[1] Fiedler B, Gojny FH, Wichmann MHG, Nolte MCM, Schulte K. Fundamental aspects of nano-reinforced composites. Compos Sci Technol 2006;66:3115–25.
[2] Gorbatikh L, Lomov SV, Verpoest I. Original mechanism of failure initiation revealed through modelling of naturally occurring microstructures. J Mech Phys Solids 2010;58:735–50.
[3] Lomov SV, Huysmans G, Verpoest I. Hierarchy of textile structures and architecture of fabric geometric models. Text Res J 2001;71(6):534–43.
[4] Verpoest I, Lomov SV. Virtual textile composites software Wisetex: integration with micro-mechanical. permeability and structural analysis. Compos Sci Technol 2005;65(15–16):2563–74.
[5] Qian H, Greenhalgh ES, Shaffer MSP, Bismarck A. Carbon nanotube-based hierarchical composites: a review. J Mater Chem 2010;20:4751–62.
[6] Chou TW, Gao LM, Thostenson ET, Zhang ZG, Byun JH. An assessment of the science and technology of carbon nanotube-based fibers and composites. Compos Sci Technol 2010;70(1):1–19.
[7] Garcia EJ, Wardle BL, Hart AJ, Yamamoto N. Fabrication and multifunctional properties of a hybrid laminate with aligned carbon nanotubes grown in situ. Compos Sci Technol 2008;68(9):2034–41.
[8] Blanco J, Garcia EJ, De Villoria RG, Wardle BL. Limiting mechanisms of mode I interlaminar toughening of composites reinforced with aligned carbon nanotubes. J Compos Mater 2009;43(8):825–41.
[9] Chen ZR, Ye L, Kruckenberg T. A micromechanical compaction model for woven fabric preforms. Part I: Single layer. Compos Sci Technol 2006;66(16):3254–62.
[10] Chen B, Cheng AH-D, Chou T-W. A nonlinear compaction model for fibrous preforms. Composites A 2001;32:701–7.
[11] .Gutowski TG, Kingery J, Boucher D. Experiments in composites consolidation: fiber deformation. In Annual technical conference of the society of plastic engineers, Brookfield; 1986. p. 1316–20.
[12] Lomov SV, Verpoest I. Compression of woven reinforcements: a mathematical model. J Reinforced Plast Compos 2000;19(16):1329–50.
[13] Lomov SV, Verpoest I, Peeters T, Roose D, Zako M. Nesting in textile laminates: Geometrical modelling of the laminate. Compos Sci Technol 2002;63(7):993–1007.
[14] Grishanov SA, Lomov SV, Harwood RJ, Cassidy T, Farrer C. The simulation of the geometry of two-component yarns. Part I. The mechanics of strand compression: simulating yarn cross-section shape. J Text Inst 1997;88(2):118–31. part 1.
[15] Chandrasekaran VCS, Advani S, Santare MH. Role of processing on interlaminar shear strength enhancement of epoxy/glass fiber/multi-walled carbon nanotube hybrid composites. Carbon 2010;48:3692–9.
[16] Lomov SV, Barburski M, Stoilova T, Verpoest I, Akkerman R, Loendersloot R, et al. Carbon composites based on multiaxial multiply stitched preforms. Part 3: Biaxial tension, picture frame and compression tests of the performs. Composites A 2005;36:1188–206.
[17] Yurgartis SW, Morey K, Jortner J. Measurement of yarn shape and nesting in plain-weave composites. Compos Sci Technol 1993;46:39–50.
[18] Ivanov DS, Lomov SV, Baudry F, Xie H, Van Den Broucke B, Verpoest I. Failure analysis of triaxial braided composite. Compos Sci Technol 2009;69:1372–80.
[19] Potluri P, Sagar TV. Compaction modelling of textile preforms for composite structures. Compos Struct 2008;86(1–3):177–85.
[20] Chen ZR, Ye L. A micromechanical compaction model for woven fabric preforms. Part II: Multilayer. Compos Sci Technol 2006;66(16):3263–72.
[21] Chen B, Chou T-W. Compaction of woven-fabric preforms: nesting and multi-layer deformation. Compos Sci Technol 2000;60:2223–31.
[22] Saunders RA, Lekakou C, Bader MG. Compression and microstructure of fibre plain woven cloths in the processing of polymer composite. Composites A 1998;29A:443–54.
[23] Pearce N, Summerscales J. The compressibility of a reinforcement fabric. Compos Manuf 1995;6(1):15–21.
[24] Saunders RA, Lekakou C, Bader MG. Compression and processing of polymer composite. 1. A mechanical and microstructural study for different glass fabrics and resins. Compos Sci Technol 1999;59:983–93.
[25] Lomov SV, Verpoest I, Barburski M, Laperre J. Carbon composites based on multiaxial multiply stitched preforms. Part 2: KES-F characterisation of the deformability of the preforms at low loads. Composites A 2003;34(4):359–70.
[26] Hoes K, Sol H, Dinescu D, Lomov SV, Parnas R. Study of nesting induced scatter of permeability values in layered reinforcement fabrics. Composites A 2004;35(12):1407–18.
[27] Hale RD, Villa M. Influence of opposing wave nesting in compression-loaded composites. J Compos Mater 2003;37(13):1149–66.
[28] Ito M, Chou T-W. An analytical and experimental study of strength and failure behaviour of plain weave composites. J Compos Mater 1998;32(1):2–30.
[29] .Ivanov DS, Lomov SV, Ivanov SG, Verpoest I. Damage in textile laminates of various inter-ply shift. In: Proceedings of the 14th European conference on composite materials (ECCM-14), Budapest; 2010 [CD edition].
[30] Ivanov DS, Lomov SV, Ivanov SG, Verpoest I. Stress distribution in outer and inner plies of textile laminates and novel boundary conditions for unit cell analysis. Composites A 2010;41(4):571–80.
[31] Lomov SV, Gorbatikh L, De Greef N, Karahan M, Godara A, Mezzo L, et al. Nano-engineered fibre reinforced composite: gain in properties and limitations of the manufacturing. In: Proceedings of the 14th European conference on composite materials (ECCM-14), Budapest; 2010 [CD edition].

[32] Lomov SV, Beyers L, Gorbatikh L, Verpoest I, Koissin V, Kotanjac Z, et al. Permeability and compressibility of CNT-CNF grafted textile reinforcement. In: Tenth international conference on flow processes in composite materials (FPCM-10), Ascona, Switzerland; 2010 [CD edition].
[33] Barclay RB, Bonfield W. Carbon fibre/nickel compatibility. J Mater Sci 1971;6:1076–83.
[34] Warren R, Anderson CH, Carlsson M. High-temperature compatibility of carbon fibres with nickel. J Mater Sci 1978;13:178–88.
[35] Jackson PW, Marjoram JR. Compatibility studies of carbon fibres with nickel and cobalt. J Mater Sci 1970;5:9–23.
[36] De Riccardis MF, Carbone D, Makris TD, Giorgi R, Lisi N, Salernitano E. Anchorage of carbon nanotubes grown on carbon fibres. Carbon 2006;44(4):671–4.
[37] Thostenson ET, Li WZ, Wang DZ, Ren ZF, Chou TW. Carbon nanotube/carbon fiber hybrid multiscale composites. J Appl Phys 2002;91(9):6034–7.
[38] Yakobson BI, Couchman LS. Persistence length and nanomechanics of random bundles of nanotubes. J Nanoparticle Res 2006;8(1):105–10.
[39] Lomov SV, Koissin V, Karahan M, Godara A, Gorbatikh L, Verpoest I. Compressibility of CNT-grafted fibrous reinforcements: a theory. Int J Mater Form 2010;3:627–30.